Supporting information for

Highly efficient 2D siloxene coated Ni foam catalyst for methane dry reforming and an effective approach to recycle spent catalyst towards energy application

Karthikeyan Krishnamoorthy[1], Sudhakaran M. S. P.[2], Parthiban Pazhamalai[3], Vimal Kumar Mariappan[3], Young Sun Mok[2], Sang -Jae Kim[3,4*]

[1]Nanomaterials laboratory, Department of Mechanical Engineering, Jeju National University, Jeju 63243, South Korea.

[2]Department of Chemical and Biological Engineering, Jeju National University, Jeju 63243, South Korea

[3]Department of Mechatronics Engineering, Jeju National University, Jeju 63243, South Korea.

[4]Department of Advanced Convergence Science & Technology, Jeju National University, Jeju 63243, South Korea.

[#] These authors contributed equally in this work

[*]Corresponding author Email: kimsangj@jejunu.ac.kr

S1. Experimental section

S1.1 Materials

Calcium silicide ($CaSi_2$) was obtained from Kojundo Chemicals Laboratory Co. Ltd., Japan. Hydrochloric acid (HCl), carbon black, and N-Methyl-2-pyrrolidone(NMP) were obtained from Dae-Jung Chemicals Ltd, South Korea. Polyvinylidene fluoride (PVDF) was purchased from Sigma Aldrich Ltd., South Korea. The electrolyte tetraethylammonium tetrafluoroborate ($TEABF_4$) was purchased from Alfa Aesar Chemicals, South Korea. The Ultrasound irradiation was carried out in a VCX 750 ultrasonicator (Sonics and Materials, Inc, USA, (20 kHz, 750 W)) using a direct-immersion titanium horn. Methane (CH_4), carbon dioxide (CO_2), carbon monoxide (CO), hydrogen (H_2), and Argon (Ar) high purity (99.9%) gases were purchased from P S Chem. Co. Ltd., South Korea. The carbon deposited siloxene/Ni foam spent catalyst is uses as electrodes for the fabrication of a symmetric supercapacitor device.

S1.2 Preparation of siloxene sheets

The 2D siloxene sheets was prepared via topochemical transformation of calcium silicide in an ice-cold hydrochloric acid [1–3]. Briefly, to synthesize siloxene sheets, $CaSi_2$ powders (1 g) were stirred in concentrated HCl (100 mL) at 0 °C for 4 days. The transformation from black color to green color confirms the dissolution of calcium in the HCl solution. Upon completion of the reaction, the obtained green colored siloxene sheets was washed with acetone and water. The washed powder was dispersed in water (100 mL) and subjected to ultrasound irradiation for 1 h. Again, the siloxene sheets were washed with water and allowed to dry at 80 °C for 12 h.

S1.3 Preparation of siloxene/Ni foam

The siloxene sheets were coated on the surface of nickel foam via a slurry coating process as reported in our earlier work [4]. Here, the siloxene powders and PVDF were taken in the ratio

95:5 and grounded well in an agate mortar using NMP as dispersant until a uniform slurry was obtained. After that, the slurry was coated onto either side of the nickel foam via dip casting method.

S1.4 Instrumentation

The functional groups in siloxene sheet were examined using FT-IR spectroscopy (Thermo Scientific FT-IR spectrometer (Nicolet 6700)). Raman spectra were obtained using a LabRam HR Evolution Raman spectrometer (Horiba Jobin-Yvon, France). The chemical state of elements in the siloxene sheet was analyzed using X-ray photoelectron spectrometer (ESCA-2000, VG Microtech Ltd.). The surface morphology and elemental mapping analysis was examined using field-emission scanning electron microscopy (TESCAN, MIRA3) and high-resolution transmission electron microscopy (JEM-2011, JEOL).

S1.5. Dry reforming reaction of methane:

The DRM was carried out in a typical thermo-catalytic packed bed reactor (given in Figure S2). The 16 mm outer diameter of cut nickel foam were used as a support in DRM activity test, 10 wt% of siloxene/Ni foams were stacked one over one and made up to the weight of 1g, which was placed into the center of the quartz tube. The catalyst was placed tubular furnace (DS 6200) equipped with K-type thermocouple to monitor and control the temperature of the furnace. The temperature operation was controlled by a tubular furnace with a proportional-integral controller (PID controller) (DTF-50300, Daeheung Science Co., Korea). The ratio of CH_4 and CO_2 was fixed at one according to the stoichiometric reaction of DRM. The reactant gases were fed into the reactor at a ratio of 10:10:80 (CH_4: CO_2: Ar). The total feed gas was fixed at 100 mL/min, which include 10 mL of CH_4, 10 mL of CO_2 and Ar as balance. The feed gases introduced by a set of mass flow controller (MFC; MKS1179A, USA; AFC500, Atovac Co., Korea) throughout the

reaction. The catalytic activity of the prepared catalyst was examined at a temperature range of 750 °C to 900 °C at 50°C interval under atmospheric pressure. The gas chromatograph (GC) (DS Science 6200; HayeSep-Q column) was calibrated with different concentration of each gas to evaluate the calibration curve of each gas at optimized GC method, which was equipped with thermal conductivity detector (TCD). The concentration of the reactant and product gases was measured after attaining the saturation time (45 min) at the set reaction temperature. The conversion X_A of CH_4 and CO_2 of inlet and outlet gases was determined using the provided relations[5,6].

$$X_A\,(\%) = \frac{C_{A_0} - C_A}{C_{A_0} + \varepsilon_A C_A} \times 100 \qquad (1)$$

$$\varepsilon_A = \frac{\eta_{X_{A=1}} - \eta_{X_{A=0}}}{\eta_{X_{A=0}}} \qquad (2)$$

$$\frac{H_2}{CO} = \frac{F_{H_2}}{F_{CO}} \qquad (3)$$

Here, X_A is the conversion of CH_4 and CO_2, C_{A0}, and C_A are inlet and outlet concentration of reactants CH_4 and CO_2, respectively, and ε_A is the fractional change in the volumetric flow rate of the reaction. The $\eta_{X_{A=0}}$ is the total number of moles of reactants (no conversion) while $\eta_{X_{A=1}}$ is the total number of moles of products (complete conversion). For the feed gas composition of 10/10/80 (CH_4/CO_2/Ar), εA is calculated to be 0.2. The F_{H2} and F_{CO} molar flow rate of H_2 and CO in the outlet.

The kinetics of the siloxene/Ni catalyst was examined by varying the partial pressure of the reactants. The kinetic study for the 10.0 wt. % of siloxene/Ni catalyst was carried out under the variable partial pressures of CH_4 and CO_2. The rate of reaction is the effect of partial pressure and the corresponding rate law equation can be expressed as follow,

$$r_{H_2} = \frac{a\left(P_{CH_4} P_{CO_2} - \frac{P_{CO}^2 P_{H_2}^2}{K_c}\right)}{1 + b\,P_{CH_4} + c\,P_{CO_2}} \quad (4)$$

Here, the $"r_{H_2}"$ - rate of reaction H_2, $"P_{CH_4}"$ - partial pressure of CH_4, $"P_{CO_2}"$ - partial pressure of CO_2, $"P_{CO}"$ - partial pressure of CO, $"P_{H_2}"$ - partial pressure of H_2, $"K_c"$ – equilibrium rate constant, and "a & b" are the coefficients of CH_4, and "c" is the coefficients of CO_2, respectively.

2.6 Reusability of the carbon/siloxene/Ni spet catalyst as electrodes for supercapacitors: Fabrication and electrochemical testing

The carbon deposited siloxene/Ni foam electrodes are used for the fabrication of a symmetric supercapacitor device using the method reported in earlier works[7]. The carbon/siloxene/Ni supercapacitor was fabricated in a CR2032 coin cell configuration separated by a Celgard membrane. A 1M $TEABF_4$ is used as the electrolyte. The fabricated supercapacitor device was crimped using an electric coin cell crimping and disassembling machine (MTI, Korea). All the electrolyte handling and device fabrication were carried out in a glove box with less than 1 ppm of moisture and oxygen. Electrochemical characterization of the carbon/siloxene/Ni supercapacitor were analyzed using cyclic voltammetry (CV) at various scan rates, EIS analysis in the frequency range from 0.01 Hz to 100 kHz at an amplitude of 10 mV, and galvanostatic

charge-discharge (CD) measurements using different current ranges were performed using an Autolab PGSTAT302N electrochemical workstation.

The specific capacitance (C), energy (E) and power (P) density of the carbon/siloxene/Ni supercapacitor was determined according to the following relations [8–10]:

$$C_G = (I \times T_d) / (M \times \Delta V) \text{……...…. (5)}$$

$$E = [C \times \Delta V^2] / 2 \text{ ……..……(6)}$$

$$P = E / T_d \text{ ……...……(7)}$$

Here *"C"* represents the specific gravimetric device capacitance (F g^{-1}), *"I"* is the discharge current, *"T_d"* is the time required for discharge, *"M"* is the electroactive mass loading of active materials in the electrode and *"ΔV"* is the operating voltage window, *"E"* and *"P"* are the energy and power density of the supercapacitor.

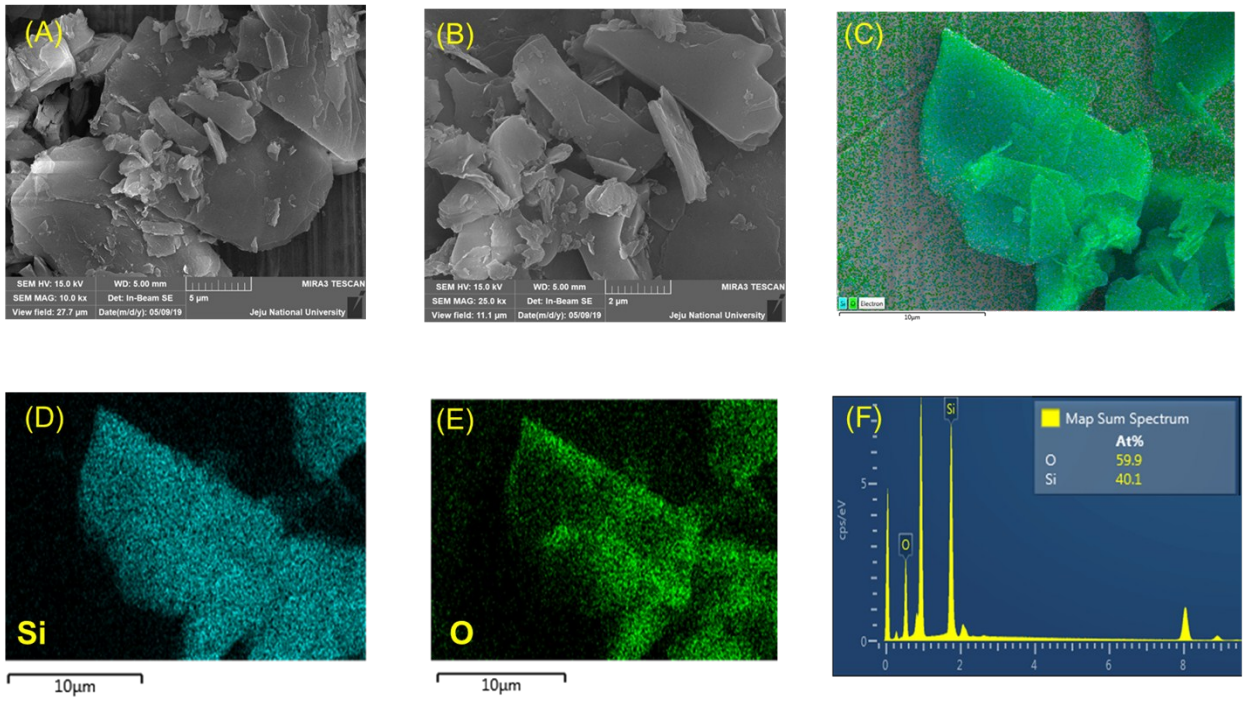

Figure S1. (A-B) FESEM micrograph of siloxene sheets. Elemental mapping analysis of siloxene sheets (C) overlay micrograph, and (D-E) represents the elemental maps of Si, and O elements. (F) EDX spectrum of siloxene sheets.

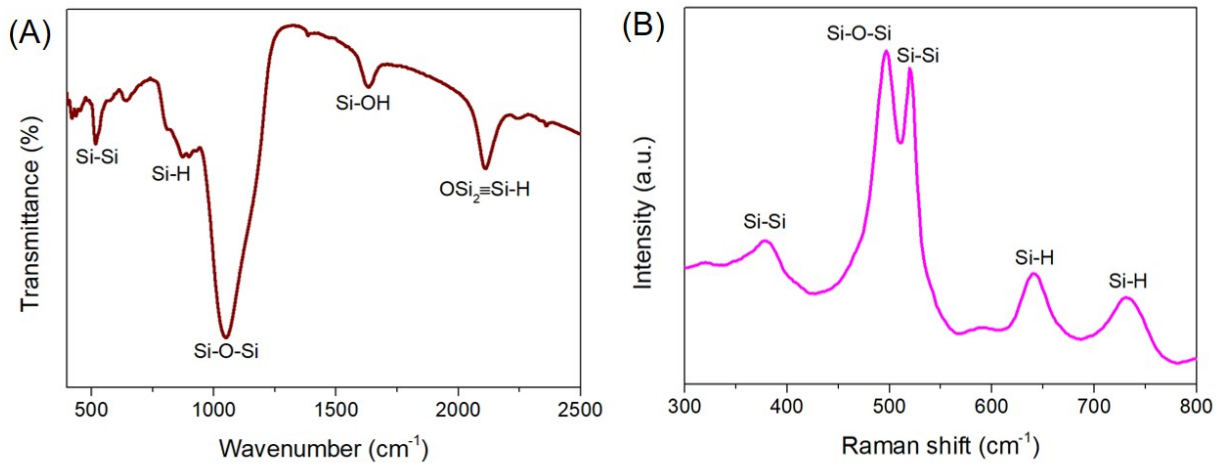

Figure S2. Physico-chemical characterizations of siloxene sheets prepared via topochemical route. (A) Fourier transform infra-red spectrum, and (B) laser Raman spectrum of siloxene sheets.

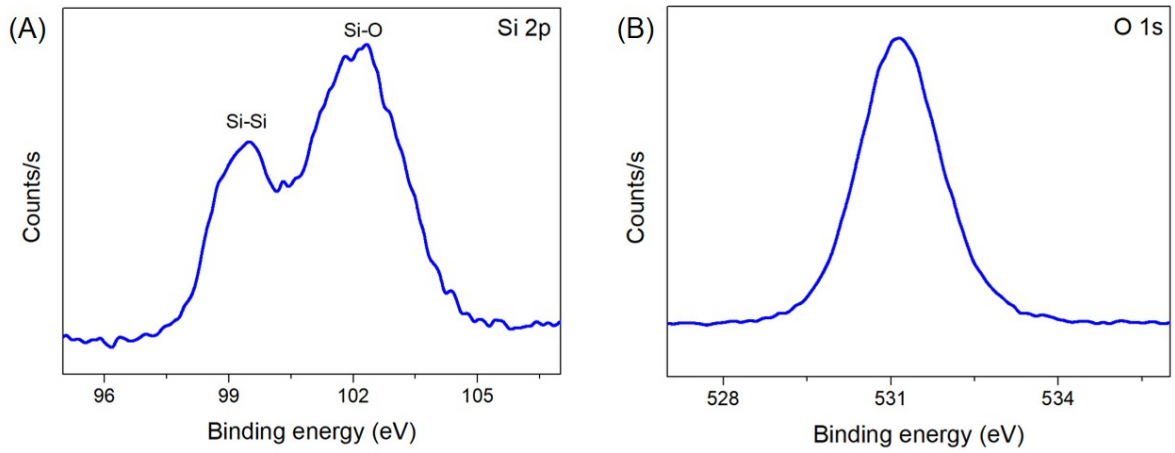

Figure S3. X-ray photoelectron spectroscopy of siloxene sheets. (A) Si 2p core level spectrum and (B) O 1s core-level spectrum of siloxene sheets.

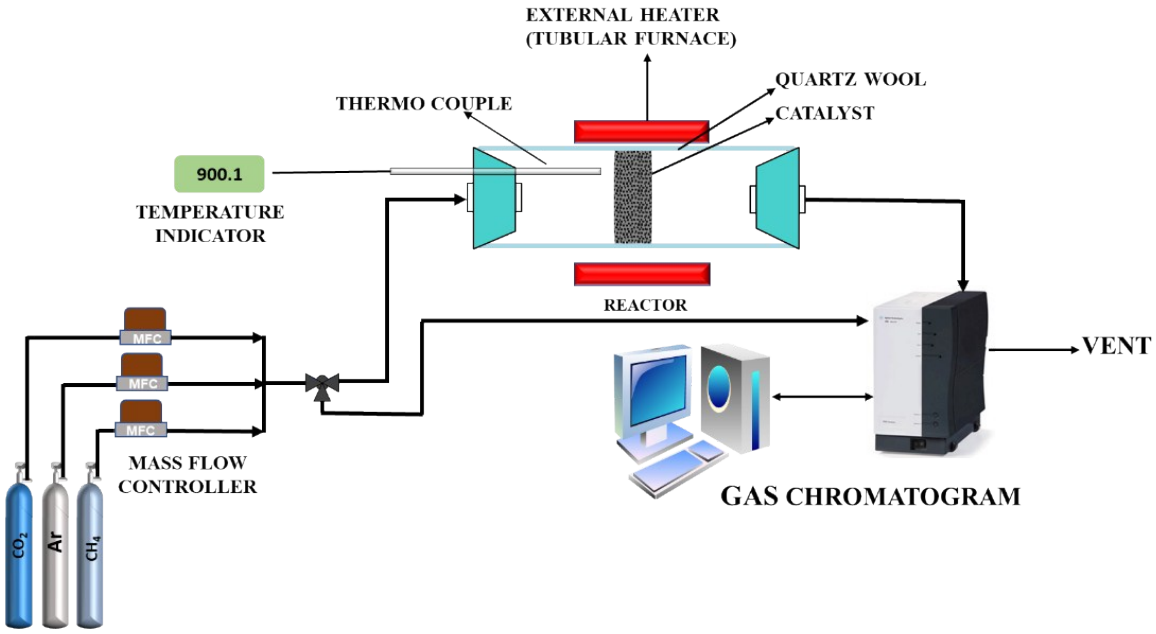

Figure S4. Experimental setup used for the DRM process.

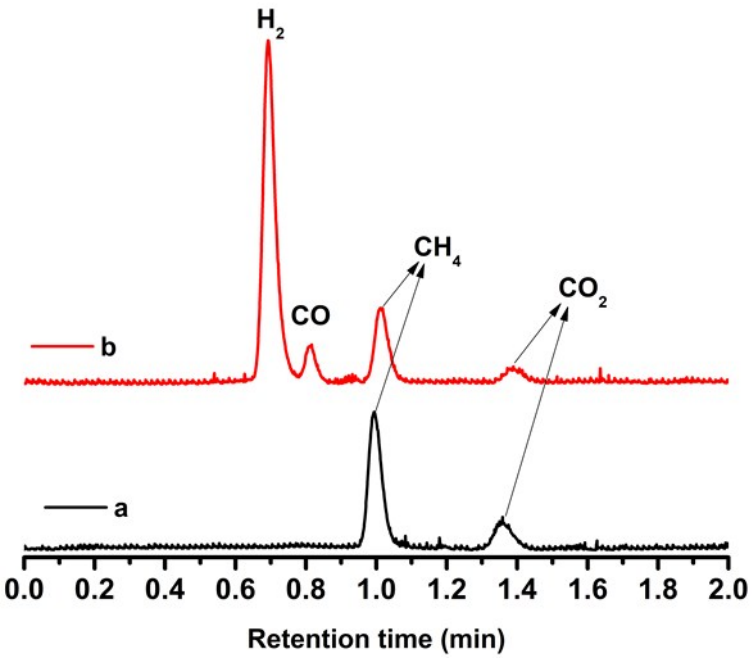

Figure S5. The gas chromatographic profiles of gas samples (a) without catalysts and (b) during DRM reaction catalyzed using siloxene/Ni foam catalyst.

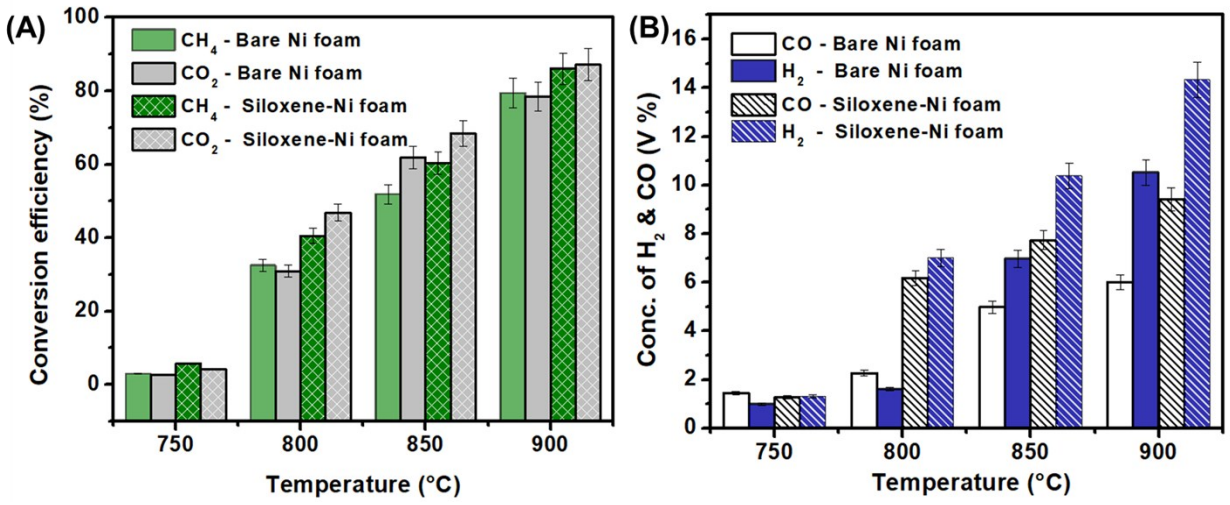

Figure S6. Comparative catalytic performance of bare Ni foam and siloxene/Ni catalyst for DRM reaction. (A) Conversion efficiencies of methane and carbon dioxide (CO_2) as a function of temperature, (B) Concentration of produced synthetic gas as a function of temperature.

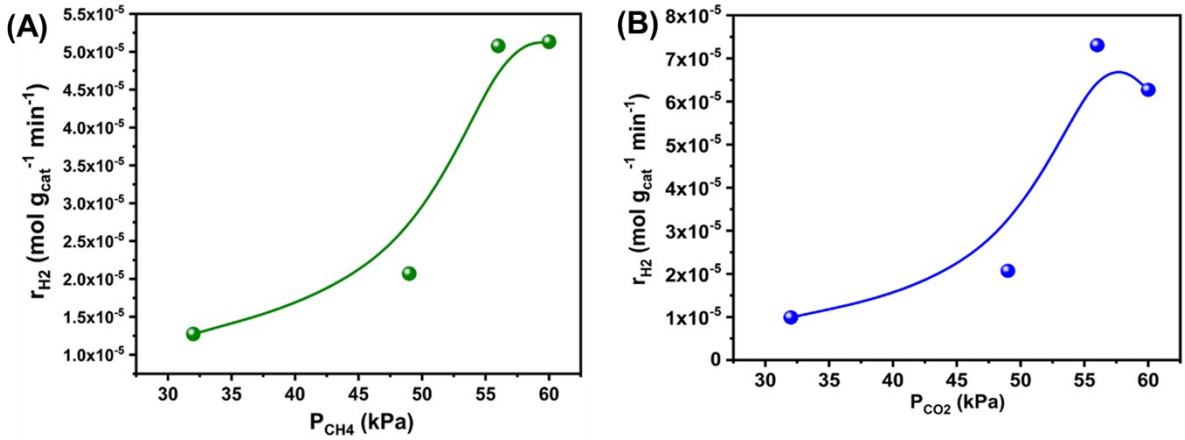

Figure S7. Effect of partial pressure of (A) CH_4 and (B) CO_2 on the rate of formation of H_2 at 1073K

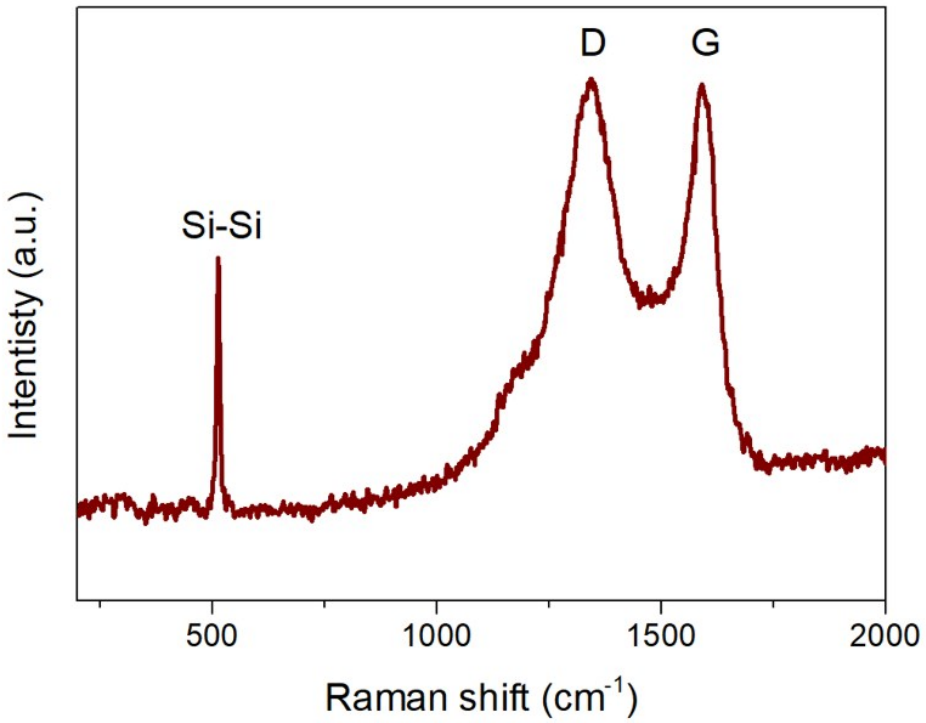

Figure S8. Laser Raman spectrum of siloxene/Ni catalyst after DRM process.

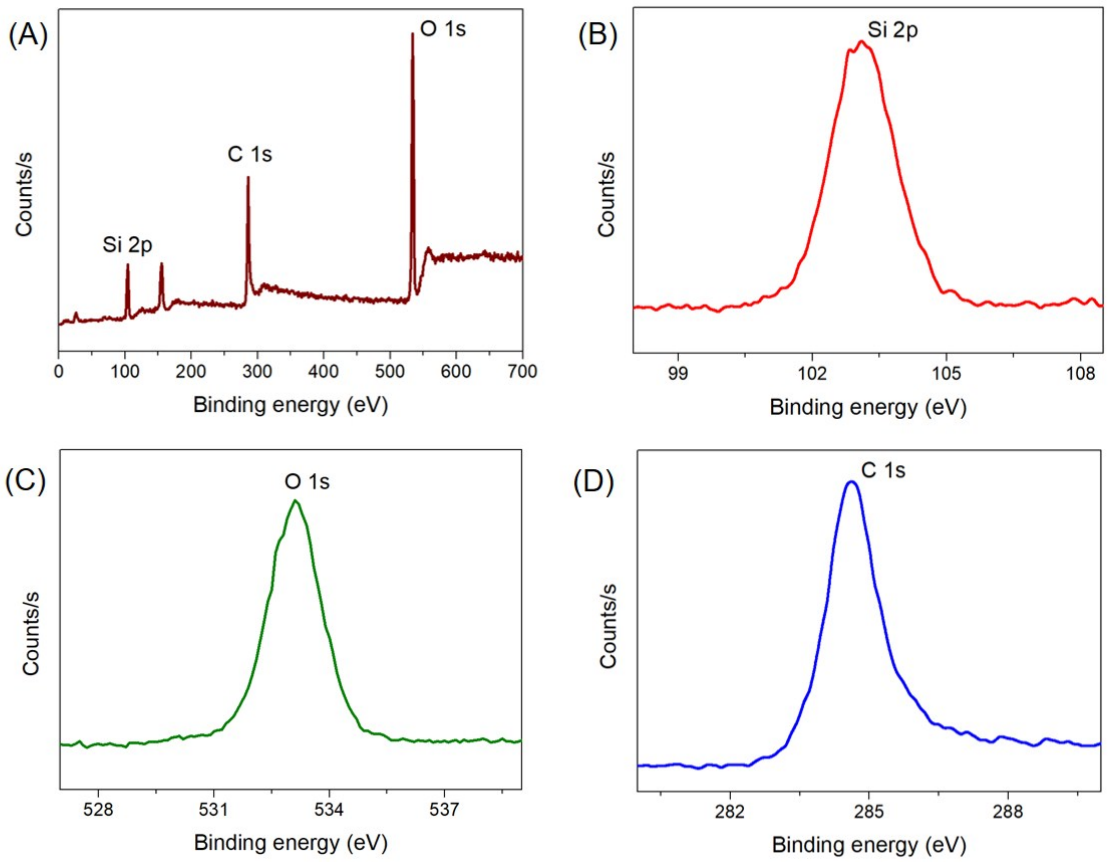

Figure S9. (A) Typical X-ray photoelectron survey spectrum of siloxene/Ni catalyst after DRM process. (B) Si 2p core-level spectrum, (C), O 1s core-level spectrum and (D) C 1s core-level spectrum of siloxene/Ni catalyst after DRM process.

Table S1: The catalytic performance and selectivity of bare Ni foam and siloxene/Ni catalyst for DRM reaction temperature at 900°C.

Catalyst	Conversion (%)		Selectivity (%)	
	X_{CH_4}	X_{CO_2}	S_{CO}	S_{H_2}
Bare Nickel foam	79	78	79	89
Siloxene/Ni	86	87	94	99

The selectivity(S) of the hydrogen (S_{H_2}) and carbon monoxide (S_{CO}) was evaluated by the following equations[6]:

$$S_{H_2} = \frac{[H_2]_{out} \cdot F_{out} \left(\frac{ml}{min}\right)}{2.\left([CH_4]_{in} \cdot F_{in} - [CH_4]_{out} \cdot F_{out}\right) \left(\frac{ml}{min}\right)} \quad (7)$$

$$S_{CO} = \frac{[CO]_{out} \cdot F_{out} \left(\frac{ml}{min}\right)}{\left([CH_4]_{in} + [CO_2]_{in}\right) \cdot F_{in} - \left([CH_4]_{out} + [CO_2]_{out}\right) \cdot F_{out} \left(\frac{ml}{min}\right)} \quad (8)$$

Here, $[CH_4]$ and [CO] are concentration of intel and outlet of reactor, $[H_2]$ and [CO] are the outlet concentration of reaction at respective reaction temperature. F is the flow rate of intel and outlet of the reactor.

Table S2: Performance metrics of the carbon/siloxene/Ni (spent catalyst) based SSC with reported carbon based SSCs using non-aqueous electrolytes.

S. No.	SSC Device	Electrolyte	OVW (V)	E (Wh Kg^{-1})	P (W Kg^{-1})	Ref
1.	Activated carbon	BMPY TFSI	3	25	100	[11]
2.	Activated carbon	PYR13-FSI	2.5	16	1110	[12]
3.	Porous carbon	EMI-BF_4	2.0	17	~750	[13]
4.	Biomass derived carbon	$TEABF_4$	2.5	~15	~300	[14]
4.	Super 30, Norit	Azp_{16} TFSI	3.5	~19	~1700	[15]
5.	RGO-CMK-5	$LiPF_6$	2.2	23.1	200	[16]
6.	Siloxene	$TEABF_4$	3.0	5.08	375	[3]
7.	HT-siloxene	$EMIMBF_4$	3.0	6.64	375	[7]
8.	rGO	$[SET_3][TFSI]$	2.5	17.7	875	[17]
9.	Graphene-P-Si	$EMIBF_4$	2.7	~10	650	[18]
10.	Graphene	$BMIBF_4$	4.0	16.5	1600	[19]
11.	Maxwell (commercial)	-	2.7	4.45	900	[20]
12.	Panasonic (commercial)	-	2.5	2.3	514	[20]
13.	Carbon/siloxene/Ni SSC	$TEABF_4$	3.0	30.81	625	This work

References:

1 H. Nakano, M. Ishii and H. Nakamura, *Chem. Commun.*, 2005, **2**, 2945.

2 S. Yamanaka, H. Matsu-ura and M. Ishikawa, *Mater. Res. Bull.*, 1996, **31**, 307–316.

3 K. Krishnamoorthy, P. Pazhamalai and S. J. Kim, *Energy Environ. Sci.*, 2018, **11**, 1595–1602.

4 G. K. Veerasubramani, K. Krishnamoorthy, R. Sivaprakasam and S. J. Kim, *Mater. Chem. Phys.*, 2014, **147**, 836–842.

5 Y. S. Mok, E. Jwa and Y. J. Hyun, *J. Energy Chem.*, 2013, **22**, 394–402.

6 S. M.S.P, L. Sultana, M. M. Hossain, J. Pawlat, J. Diatczyk, V. Brüser, S. Reuter and Y. S. Mok, *J. Ind. Eng. Chem.*, 2018, **61**, 142–151.

7 P. Pazhamalai, K. Krishnamoorthy, S. Sahoo, V. K. Mariappan and S. J. Kim, *ACS Appl. Mater. Interfaces*, 2019, **11**, 624–633.

8 P. Yu, W. Fu, Q. Zeng, J. Lin, C. Yan, Z. Lai, B. Tang, K. Suenaga, H. Zhang and Z. Liu, *Adv. Mater.*, 2017, **29**, 1701909.

9 L. Yao, Q. Wu, P. Zhang, J. Zhang, D. Wang, Y. Li, X. Ren, H. Mi, L. Deng and Z. Zheng, *Adv. Mater.*, 2018, **30**, 1706054.

10 S. Zhang and N. Pan, *Adv. Energy Mater.*, 2015, **5**, 1401401.

11 Z. Li, J. Liu, K. Jiang and T. Thundat, *Nano Energy*, 2016, **25**, 161–169.

12 A. Eftekhari, *Energy Storage Mater.*, 2017, **9**, 47–69.

13 W. Lu, K. Henry, C. Turchi and J. Pellegrino, *J. Electrochem. Soc.*, 2008, **155**, A361.

14 X. Wang, Y. Li, F. Lou, M. E. Melandsø Buan, E. Sheridan and D. Chen, *RSC Adv.*, 2017, **7**, 23859–23865.

15 S. Pohlmann, T. Olyschläger, P. Goodrich, J. Alvarez Vicente, J. Jacquemin and A. Balducci, *J. Power Sources*, 2015, **273**, 931–936.

16 Z. Lei, Z. Liu, H. Wang, X. Sun, L. Lu and X. S. Zhao, *J. Mater. Chem. A*, 2013, **1**, 2313.

17 N. das M. Pereira, J. P. C. Trigueiro, I. de F. Monteiro, L. A. Montoro and G. G. Silva, *Electrochim. Acta*, 2018, **259**, 783–792.

18 S. Chatterjee, R. Carter, L. Oakes, W. R. Erwin, R. Bardhan and C. L. Pint, *J. Phys. Chem. C*, 2014, **118**, 10893–10902.

19 Y. Chen, X. Zhang, D. Zhang and Y. Ma, *Mater. Lett.*, 2012, **68**, 475–477.

20 A. Burke, *Electrochim. Acta*, 2007, **53**, 1083–1091.